Interference mitigation in multicell LTE systems: performance over correlated fading channels

Daniele Molteni and Monica Nicoli
Dip. di Elettronica e Informazione, Politecnico di Milano, Piazza L. da Vinci 32, I-20133 Milano, Italy
e-mail: {molteni,nicoli}@elet.polimi.it

***Abstract*— We consider a multicell multiple-input-multiple-output (MIMO) orthogonal-frequency-division-multiple-access (OFDMA) scenario conforming to the 3GPP Long Term Evolution (LTE) recommendation. Scheduling policies proposed for interference mitigation in LTE rely on a pseudo-random permutation of the subcarriers (interference randomization) or on a centrally coordinated reuse of the OFDMA bandwidth (interference coordination). For both the approaches, this paper investigates the performance of a multiple antenna communication over a Rayleigh fading multipath channels. An analytical model is derived to assess the average bit error probability for frequency-selective (correlated) channels with either stationary or non-stationary (due to subcarrier permutation) multicell interference. Simulation results corroborate the proposed analytical model for different traffic conditions and propagation scenarios.**

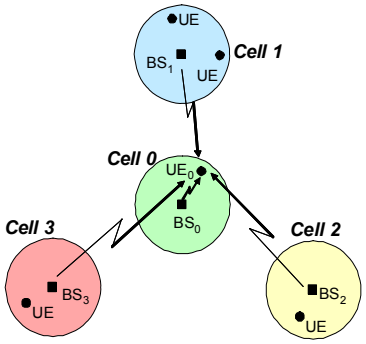

Fig. 1. Multi-cell interference scenario in downlink transmission.

I. Introduction

The 3GPP Long Term Evolution (LTE) [1]-[2] is in process of standardization for future broad band wireless communication systems. Orthogonal frequency division multiple access (OFDMA) and multiple-input multiple-ouput (MIMO) technologies have been proposed for the downlink transmission of the LTE system in order to cope with multipath fading and interference impairments [3]. Due to the limited amount of radio resources, frequencies are supposed to be reused in a multicell scenario, thus generating co-cell interference among users sharing the same frequency band. To reduce such a performance degradation some interference mitigation techniques are currently under evaluation, referred to as interference cancellation, interference coordination and interference randomization. The first approach aims at reducing the interference effects by spatial filtering (beamforming) and requires the use of antenna arrays [4]. Interference coordination is based on a coordinated access to the radio resource among the active users of nearby cells so as to avoid (as far as possible, i.e., for moderate traffic load) inter-cell interference. On the other hand, the interference randomization policy spreads the data all over the bandwidth by subcarrier permutation so as to randomize the interference and achieve frequency diversity.

Due to the key role of interference mitigation in LTE multicell systems, works have been recently carried out to evaluate the impact of the above scheduling policies on the system performance. Focusing on the coordination strategy, [5] investigates different reuse partitioning techniques obtaining symbol and packet error rate at the link level. Ref. [6] analytically assesses the bit-error-rate (BER) of an LTE system over flat-fading channels, comparing the interference coordination and permutation approaches. In this paper we extend the analysis to MIMO transmission over realistic frequency-selective fading environments. The performance is evaluated in terms of BER at the output of the forward error correction (FEC) decoder, averaging over the fading channel and the interference configuration. The analytical tools [4] are exploited to cope with the correlation of the channel response over the frequency domain, while the collision model [6] allows to account for the varying interference scenario. The system performance is here derived for a MIMO-OFDMA link, taking into account the spatial diversity introduced by the multi-antenna framework, in either stationary (as for interference coordination) or non-stationary (as for interference permutation) interference. The analytical performance is finally validated by numerical simulations of an LTE system in realistic propagation scenarios.

This work is supported by MIUR-FIRB Integrated System for Emergency (InSyEme) project under the grant RBIP063BPH.

II. Modeling the 3GPP LTE system

A. Multicell OFDMA layout

We consider the downlink channel of a MIMO-OFDMA multicell system modelled according to the 3GPP LTE recommendation [1]-[2]. Base stations (BSs) are distributed over the access area forming a cellular layout as exemplified in Fig. 1. Within each cell, a BS provided with N_T transmitting antennas serves a number of user equipments (UEs) having N_R receiving antennas each. Multiple access is handled through OFDMA: the common channel resource is organized in time-frequency units (chunks), each consisting of a set of K_C adjacent subcarriers over K_S subsequent OFDM symbols. The maximum number of chunks that can be allocated over the

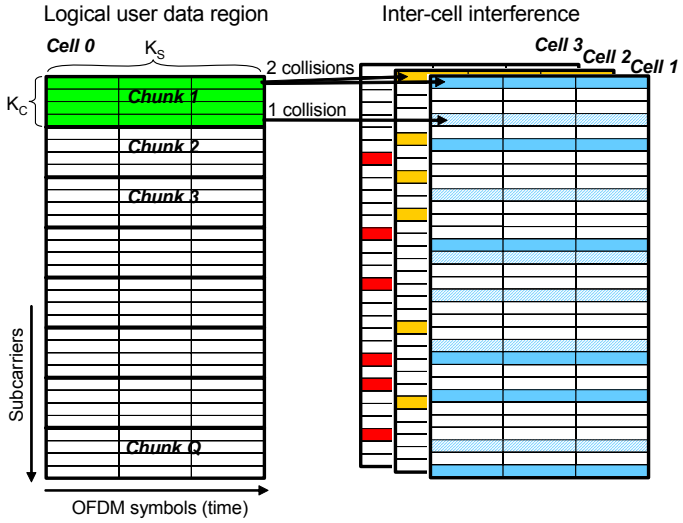

Fig. 2. Example of interference scenario for the multi-cell layout in Fig. 1 with randomization mode. The interference configuration varies from subcarrier to subcarrier due to random permutation.

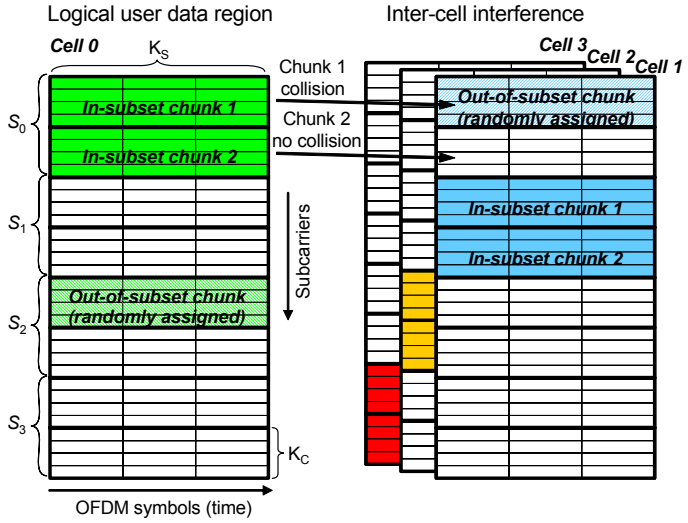

Fig. 3. Example of interference scenario for the multi-cell layout in Fig. 1 with coordination mode. Since the traffic load for cells 0 and 1 exceed the subset capacity ($\eta > \frac{1}{N_I+1} = \frac{1}{4}$), out-of-subset chunks generate collisions.

bandwidth is $Q = K/K_C$, where K denotes the total number of subcarriers used for data transmission. Some chunks may not be used when only few UEs are active; thereby, we define the traffic load $\eta \leq 1$ (assumed to be the same for all the cells) as the fraction of chunks that are allocated out of Q.

Due to frequency reuse, nearby cells use the same frequency bandwidth thus generating inter-cell interference. Let us consider for instance the cell 0 in Fig. 1: the transmission from BS_0 to UE_0 is impaired by interference from N_I out-of-cell base stations $\{\mathrm{BS}_i\}_{i=1}^{N_I}$ which transmit using the same frequency band as BS_0. The 3GPP LTE recommendation supports two different scheduling approaches to mitigate the effects of the interference as described in the following.

B. Scheduling techniques for interference mitigation

The *interference randomization* policy prescribes a pseudo-random permutation of the subcarriers so as to spread the data of each UE all over the bandwidth. Since the permutation rule is different for each interfering cell, this approach makes the interference pattern to vary within the chunk as for a non-stationary interference scenario. Fig. 2 exemplifies this effect for the cellular layout in Fig. 1, showing the interference generated on the cell-0 chunk-1 logical subcarriers. It can be observed that the set of UEs colliding with UE_0 changes from subcarrier to subcarrier (the traffic load is $\eta < 1$, so the number of the interferers varies from 0 up to N_I). This induced non-stationarity creates diversity against the interference, as the transmission of a strong interferer affects only a portion of the data that might be recovered by FEC coding.

The *interference coordination* technique lies upon a centrally coordinated reuse partitioning strategy. The radio resource is divided into $N_I + 1$ disjoint subsets, $\{S_0, \ldots, S_{N_I}\}$, each subset being composed of $q = Q/(N_I + 1)$ chunks and assigned to a different cell. In this way the intercell interference can be completely avoided when the system load is $\eta \leq 1/(N_I+1)$. On the other hand, when the traffic exceeds the subset capacity (i.e., for $\eta > 1/(N_I + 1)$), the BS maps the exceeding data over randomly selected chunks, causing a constant amount of interference over the whole selected chunks. An example of such situation is given in Fig. 3.

C. Signal model

Let us focus on the transmission of one chunk from BS_0 to UE_0. The information-bearing bit sequence $\{b_k\}$ is coded by a convolutional code (CC), bit-interleaved and then mapped onto the QPSK sequence $\{x_k\}$. The symbols are then transmitted over K_C subcarriers using OFDM signalling. An orthogonal space time block code (OSTBC) is employed to map the signals over the N_T antennas [7]. At the receiver, OFDM demodulation is carried out at each antenna, followed by OSTBC detection, so that the output signal on the kth subcarrier is:

$$\hat{x}_k = \sqrt{\frac{P_0}{N_T}}\,\|\mathbf{H}_k\|\,x_k + n_k, \tag{1}$$

where x_k is the transmitted symbol with energy $\mathrm{E}[|x_k|^2] = E_s$, P_0/N_T is the average transmit power per antenna (normalized so that the overall transmit power is P_0), while $\mathbf{H}_k$ is the $N_R \times N_T$ MIMO channel matrix ($\|\cdot\|$ denotes the Frobenius norm). The subcarrier index k ranges over the K_C subcarriers of the chunk. The zero-mean white complex Gaussian process $n_k \sim \mathcal{CN}(0, \sigma_k^2)$ models the background noise and the inter-cell interference. Its variance is

$$\sigma_k^2 = \sum_{i \in \mathcal{I}_k} P_i + \sigma_{\mathrm{bn}}^2 = v_k P_I + \sigma_{\mathrm{bn}}^2, \tag{2}$$

where $\mathcal{I}_k$ indicates the set of cells colliding with the user UE_0 on the subcarrier k and its cardinality $v_k = |\mathcal{I}_k| \in \{0, 1, \ldots N_I\}$ represents the number of interferers (at most one per cell). P_i is the ith interferer power, while σ_{bn}^2 is the background noise variance. To simplify the analysis, in (2)

we assumed $P_i = P_I$ for $i = 1, \ldots, N_I$; nevertheless, the analysis can be adapted to the general case of non-uniform power distribution over the interferers. As described in Sect. II-B, in case of interference randomization the set $\mathcal{I}_k$ (and thus the power σ_k^2) changes with the subcarrier index k thus making the noise process n_k non-stationary over the frequency domain. On the other hand, the interference pattern is constant within the chunk when the interference coordination policy is adopted. The SINR is defined as:

$$\gamma_k = \frac{P_0 E_s}{N_T} \frac{\|\mathbf{H}_k\|^2}{\sigma_k^2} = \frac{P_0 E_s}{N_T} \frac{\|\mathbf{H}_k\|^2}{v_k P_I + \sigma_{\text{bn}}^2}. \tag{3}$$

As regards the MIMO channel, the antenna spacing at both the transmitter and receiver arrays is assumed to be large enough so that the $N_R \times N_T$ elements of $\mathbf{H}_k$ can be considered as statistically independent of one another (the extension to the case of spatially correlated channel is straightforward). On the other hand, the channel is assumed to be correlated over the subcarriers, due to frequency-selective multipath fading. Namely, the (n_R, n_T)th link response $h_k^{(n_R,n_T)} = [\mathbf{H}_k]_{n_R,n_T}$ is modelled as the sum of the contributions over R paths, as:

$$h_k^{(n_R,n_T)} = G_k \sum_{r=1}^{R} \alpha_r \exp\left(-j2\pi \frac{k}{\bar{K}} \frac{\tau_r}{T}\right), \tag{4}$$

where, for the rth path, τ_r denotes the delay and α_r the complex fading amplitude. G_k is the frequency response of the cascade connection of the transmitter and receiver filters on the kth subcarrier, T is the sampling interval, and $\bar{K}$ is the total number of subcarriers. The R Rayleigh fading amplitudes are uncorrelated to each other. Each amplitude, $\alpha_r \sim \mathcal{CN}(0, \rho(\tau_r))$, has mean power $\rho(\tau_r)$ that follows an exponential power delay profile: $\rho(\tau) = \rho(0)\exp(-\tau/\sigma_\tau)$ with delay spread σ_τ and normalizing factor $\rho(0) = 1/\sum_{r=1}^{R} \exp(-\tau_r/\sigma_\tau)$. The channel is assumed to be constant over the time (at least within K_S symbol intervals).

We also introduce two simplified Rayleigh fading models as extreme cases of frequency selectivity (to be used for lower/upper performance bounds in Sect. IV): the frequency-flat (FF) channel where the channel gains are constant all over the bandwidth (as for $\sigma_\tau \to 0$) and the maximum frequency diversity (FD) channel where the channel gains are i.i.d. over the subcarriers (as for the ideal case of maximum σ_τ).

III. Performance analysis

According to the union bound approach, the average (with respect to the interference and the fading channel) bit error probability at the output of the CC decoder is [8]:

$$P_b = \Pr(\hat{b}_k \neq b_k) \leq \frac{1}{k_c} \sum_{d \geq d_{\text{free}}} c(d)\, P(d) \tag{5}$$

where k_c is the number of input bits for each branch of the CC trellis, d_{free} is the free Hamming distance, $c(d)$ is the number of information-bit errors for error events with Hamming weight d. The average pairwise error probability (PEP) $P(d) = P(\mathbf{x} \to \hat{\mathbf{x}})$ is the probability that the detector selects the codeword $\hat{\mathbf{x}}$ having Hamming distance d from the transmitted codeword $\mathbf{x}$. We assume that the d erroneous bits in the error event are mapped, through interleaving and scheduling, onto a set of d different subcarriers $\mathcal{F} = \{f_1, \ldots, f_d\}$; as regards the positions of the d error bits, we select the worst pattern of error positions depending on the specific code, interleaver and channel condition (see [4]).

Each average PEP in (5) depends on the SINR variates $\gamma = \{\gamma_{f_1}, \ldots, \gamma_{f_d}\}$ and the interference configurations $\mathcal{I} = \{\mathcal{I}_{f_1}, \ldots, \mathcal{I}_{f_d}\}$ that are experienced along the error event. It can thus be obtained as $P(d) = \mathrm{E}_{\gamma,\mathcal{I}}[P(d|\gamma, \mathcal{I})]$ by averaging the conditioned PEP $P(d|\gamma, \mathcal{I})$ over the fading gains γ and the interference sets $\mathcal{I}$. The conditioned PEP is

$$P(d|\gamma, \mathcal{I}) = Q\left(\sqrt{2\gamma_{\text{eff}}}\right), \tag{6}$$

where γ_{eff} denotes the effective SINR at the decision variable,

$$\gamma_{\text{eff}} = \sum_{k \in \mathcal{F}} \gamma_k = \frac{P_0 E_s}{N_T} \sum_{k \in \mathcal{F}} \frac{\|\mathbf{H}_k\|^2}{v_k P_I + \sigma_{\text{bn}}^2}, \tag{7}$$

depending on the numbers $\{v_k\}_{k \in \mathcal{F}}$ of the interferers in the sets $\{\mathcal{I}_k\}_{k \in \mathcal{F}}$. In the sequel, we first derive the average of (6) with respect to γ for a given interference scenario $\mathcal{I}$ (see Sect. III-A); then, we average over $\mathcal{I}$ (see Sect. III-B).

A. Average of the PEP over the fading channel

The average of the conditioned PEP with respect to γ is:

$$P(d|\mathcal{I}) = \mathrm{E}_\gamma\left[P(d|\gamma, \mathcal{I})\right] = \int Q\left(\sqrt{2\gamma_{\text{eff}}}\right) p(\gamma_{\text{eff}}|\mathcal{I}) d\gamma_{\text{eff}}. \tag{8}$$

where $p(\gamma_{\text{eff}}|\mathcal{I})$ is the effective SINR probability density function (pdf). For its derivation we follow the same approach as in [4] by extending the method to the MIMO channel case. Let $\tilde{\mathbf{H}}_k = \sqrt{P_0 E_s / N_T} \cdot \mathbf{H}_k / \sigma_k$ be the scaled MIMO matrix and $\mathbf{h} = \mathrm{vec}[\tilde{\mathbf{H}}_{f_1} \cdots \tilde{\mathbf{H}}_{f_d}]$ the vector that gathers all the $dN_T N_R$ scaled channel gains associated to the d subcarriers of the error event. We observe that $\mathbf{h}$ is a zero-mean complex Gaussian random vector, $\mathbf{h} \sim \mathcal{CN}(\mathbf{0}, \mathbf{R})$, with covariance $\mathbf{R} = \mathrm{E}[\mathbf{h} \cdot \mathbf{h}^{\mathrm{H}}] = \mathbf{R}_{\mathrm{F}} \otimes \mathbf{R}_{\mathrm{S}}$. Here $\otimes$ denotes the Kronecker product, $\mathbf{R}_{\mathrm{S}} = \mathbf{I}_{N_R N_T}$ accounts for the uncorrelation of the fading gains over the antennas, while $\mathbf{R}_{\mathrm{F}}$ is the $d \times d$ frequency-domain correlation matrix whose element $r_{k,h} = [\mathbf{R}_{\mathrm{F}}]_{k,h}$ represents the cross-correlation of the channel responses on the subcarriers f_k and f_h:

$$r_{k,h} = \frac{P_0 E_s}{N_T} \frac{G_{f_k} G_{f_h}^*}{\sigma_{f_k} \sigma_{f_h}} \sum_{r=1}^{R} \rho(0) \exp\left[-\frac{\tau_r}{\sigma_\tau} - j2\pi \frac{f_k - f_h}{\bar{K}} \frac{\tau_r}{T}\right]. \tag{9}$$

From (7), the effective SINR can be written as the sum of the square magnitudes of the entries of the vector $\mathbf{h}$: $\gamma_{\text{eff}} = ||\mathbf{h}||^2$. The pdf of γ_{eff} is thus a function the correlation values (9), which clearly depend on the channel coherence bandwidth $(1/\sigma_\tau)$ compared to the system bandwidth $(1/T)$ and on the interleaving pattern (the more the error-bit subcarriers f_k and f_h are spread away in the frequency domain, the lower is the correlation and the higher is the diversity).

In order to derive the effective SINR pdf, we consider the covariance matrix eigenvalue decomposition $\mathbf{R} = \mathbf{U}\mathbf{\Lambda}\mathbf{U}^{\mathrm{H}}$. Due to the Kronecker structure, the $dN_TN_R \times dN_TN_R$ eigenvalue matrix is $\mathbf{\Lambda} = \mathbf{\Lambda}_{\mathrm{F}} \otimes \mathbf{I}_{N_RN_T}$ (the spatial uncorrelation assumption makes the dN_TN_R eigenvalues to be grouped into d clusters of N_RN_T equal elements each) where $\mathbf{\Lambda}_{\mathrm{F}} = \mathrm{diag}\{\lambda_1, \ldots, \lambda_d\}$ collects the d eigenvalues of the frequency-domain correlation matrix $\mathbf{R}_{\mathrm{F}}$. The effective SINR can now be rewritten as $\gamma_{\mathrm{eff}} = ||\mathbf{b}||^2$, in terms of the channel projection $\mathbf{b} = \mathbf{U}^{\mathrm{H}}\mathbf{h}$ onto the orthonormal basis $\mathbf{U}$. Since the entries of the new vector $\mathbf{b} \sim \mathcal{CN}(\mathbf{0}, \mathbf{\Lambda})$ are uncorrelated, the moment generating function (MGF) of γ_{eff} is [9]:

$$M_{\gamma_{\mathrm{eff}}}(s) = \prod_{i=1}^{d} \frac{1}{(1-\lambda_i s)^{N_RN_T}}. \quad (10)$$

Based on the result above, the conditioned PEP (8) can be evaluated using two different approaches. As shown in [9, p. 103], we can directly integrate the MGF (10) using the integral definition of the Q function, obtaining:

$$P(d|\mathcal{I}) = \frac{1}{\pi}\int_0^{\pi/2} \prod_{i=1}^{d} \left(1 + \frac{\lambda_i}{\sin^2\theta}\right)^{-N_RN_T} d\theta. \quad (11)$$

As an alternative, we can evaluate (8) using as $p(\gamma_{\mathrm{eff}})$ the inverse Fourier transform of (10) which yields (see [10]):

$$p(\gamma_{\mathrm{eff}}|\mathcal{I}) = \prod_{n=1}^{d}\left(\frac{\bar{\lambda}}{\lambda_n}\right)^{N_RN_T} \sum_{m=0}^{\infty} \frac{\delta_m \gamma_{\mathrm{eff}}^{m+\mu-1} e^{-\gamma_{\mathrm{eff}}/\bar{\lambda}}}{\bar{\lambda}^{m+\mu}\Gamma(m+\mu)} \quad (12)$$

where $\mu = dN_RN_T$, $\bar{\lambda} = \min_n\{\lambda_n\}$ and the coefficients δ_m are obtained recursively, starting from $\delta_0 = 1$, according to

$$\delta_m = \frac{1}{m}\sum_{i=1}^{m}\left[\sum_{j=1}^{d} N_RN_T\left(1 - \frac{\bar{\lambda}}{\lambda_j}\right)^i\right]\delta_{m-i},\ m \geq 1. \quad (13)$$

B. Average of the PEP over the interference

The average of the conditioned PEP (8) with respect to the interference configuration $\mathcal{I}$ can be written as:

$$P(d) = \mathrm{E}_{\mathcal{I}}[P(d|\mathcal{I})] = \sum_{\mathbf{v}} P(d|\mathbf{v})\Pr(\mathbf{v}), \quad (14)$$

where $P(d|\mathbf{v})$ is the PEP (calculated as in Sect. III-A) conditioned to the collision numbers $\mathbf{v} = [v_{f_1} \cdots v_{f_d}]$ associated with $\mathcal{I}$, while $\Pr(\mathbf{v})$ is the collision probability depending on the traffic load η. In the sequel we derive the term $\Pr(\mathbf{v})$ for each scheduling policy following the same procedure as in [6].

1) Collision model for interference randomization: Due to pseudo-random subcarrier permutation, the number (v_k) of collisions changes with the frequency index $k \in \mathcal{F}$ and it can be reasonably considered as independent from subcarrier to subcarrier. It follows that $\Pr(\mathbf{v}) = \prod_{k=1}^{d}\Pr(v_{f_k})$, where each term $\Pr(v_{f_k})$ follows the binomial distribution:

$$\Pr(v) = \binom{N_I}{v}\eta^v(1-\eta)^{N_I-v}. \quad (15)$$

We highlight that the evaluation of (14) requires the computation of the conditioned PEP for each of the $(N_I+1)^d$ possible values of $\mathbf{v}$ (differently from [6], here also the order of the d collisions affects $P(d|\mathbf{v})$ due to the channel correlation over the frequencies). This number is excessive for any practical performance assessment. Thereby, we employ a semi-analytical approach where the expectation (14) is replaced by a Monte-Carlo average over a number of random realizations of $\mathbf{v}$ generated according to the distribution (15).

We observe that the derivation of the conditioned PEP $P(d|\mathbf{v})$ in Sect. III-A relies on perfect knowledge of the interference power σ_k^2 at the decoder (*genie decoder*). In case of interference randomization this assumption may not be realistic as the noise level changes along the frequencies and it has to be estimated on each subcarrier. On the other hand, practical receivers can measure the *average* noise power over the chunk. The BER for this more realistic receiver (*conventional decoder*) can be derived as done so far by replacing σ_k^2 in (3) and (7) with the average $\overline{\sigma_k^2} = \frac{1}{d}\sum_{k\in\mathcal{F}}\sigma_k^2 = v_{\mathcal{F}}P_I + \sigma_{\mathrm{bn}}^2$ where $v_{\mathcal{F}} = \frac{1}{d}\sum_{k\in\mathcal{F}} v_k$. The expression (14) simplifies to the average over $(N_I+1)d$ values of the scalar $v_{\mathcal{F}}$.

2) Collision model for interference coordination: In this case the number of collisions is constant over the whole chunk, so that $v_k = v$ and thus $\sigma_k^2 = vP_I + \sigma_{\mathrm{bn}}^2$, $\forall k \in \mathcal{F}$. The vector $\mathbf{v}$ in (14) reduces to the scalar v with distribution $\Pr(v)$. Under moderate cell load ($\eta \leq \frac{1}{N_I+1}$) the coordination policy guarantees that no collision occurs ($v = 0$). On the other hand, for larger traffic load ($\eta > \frac{1}{N_I+1}$, see Fig. 3) collisions may affect the transmission with probability [6]:

$$\Pr(v) = \Pr(v|\mathcal{H}_0)\Pr(\mathcal{H}_0) + \Pr(v|\mathcal{H}_1)\Pr(\mathcal{H}_1) \quad (16)$$

where $\Pr(\mathcal{H}_0) = 1/[\eta(N_I+1)]$ and $\Pr(\mathcal{H}_1) = 1 - \Pr(\mathcal{H}_0)$ are the probabilities that the chunk is assigned, respectively, inside (event $\mathcal{H}_0$) and outside (event $\mathcal{H}_1$) the subset $\mathcal{S}_0$. The distribution of v conditioned to these two different events is

$$\begin{aligned}\Pr(v|\mathcal{H}_0) &= \binom{N_I}{v}p^v(1-p)^{N_I-v},\\ \Pr(v|\mathcal{H}_1) &= \binom{N_I-1}{v-1}p^{v-1}(1-p)^{N_I-v} \quad \text{for } v \neq 0,\end{aligned}$$

with $p = \frac{\eta - 1/N_I}{1 - 1/N_I}$ denoting the probability of chunk collision and $\Pr(0|\mathcal{H}_1) = 0$.

IV. Numerical results

In this Section we validate the analytical results of Sect. III through numerical simulation of a 3GPP LTE system. The system parameters are as follows: $\bar{K} = 1024$ subcarriers, frequency bandwidth $1/T = 10$MHz, $Q = 24$ chunks each composed of $K_C = 25$ subcarriers by $K_S = 8$ OFDM symbols, $N_T = N_R = 2$ antennas, 400 bits per chunk, $N_I = 3$ interfering cells, CC with rate $R = 1/2$, generators $g = [561, 753]$ and constraint length $T = 9$. The union bound is truncated to the first two error events with distances $d = \{12, 14\}$ and Hamming weights $c(d) = \{33, 281\}$.

Figures 4-5 compare the simulated and the analytical BER vs the average SINR for the random permutation policy, with either genie (Fig. 4) or conventional (Fig. 5) decoder. The

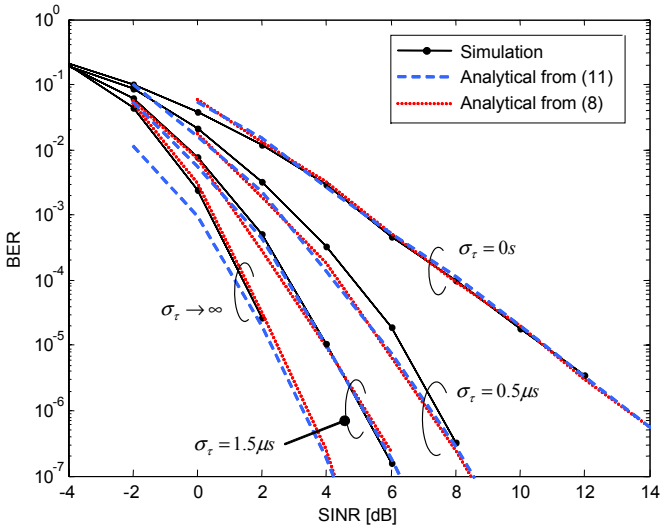

Fig. 4. Analytical and simulated BER vs SINR for a genie decoder.

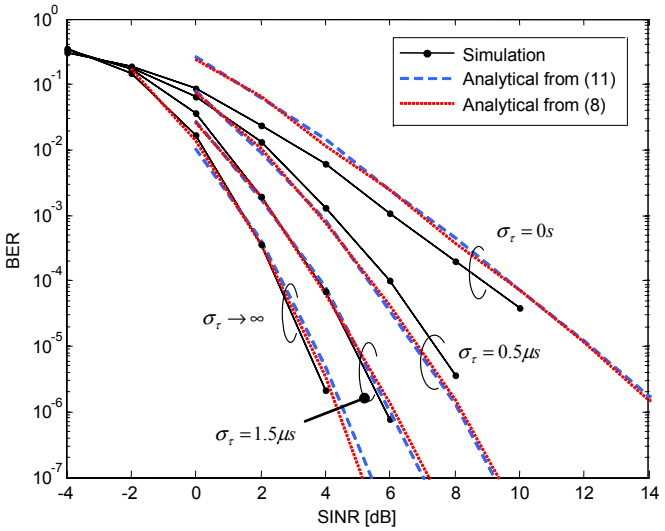

Fig. 5. Analytical and simulated BER vs SINR for a conventional decoder.

average SINR is defined as SINR$= P_0 E_s / \left(\sum_{i=1}^{N_I} P_i + \sigma^2_{\rm bn}\right)$. The analytical BER is evaluated using (8) (with (12) as SINR pdf) and (11), yielding in both cases a tight performance bound. The traffic load is $\eta = 0.4$, while the signal-to-noise ratio is fixed at SNR$= P_0 E_s/\sigma^2_{\rm bn} = 20$dB. Simulation results show that the analytical bound is less accurate for small delay spread (e.g., for $\sigma_\tau = 0.5\mu$s), as error events with large Hamming distance (not taken into account here) are more likely to occur in highly correlated channels. The performance gain of the genie receiver with respect to the conventional one is approximately 1dB.

Fig. 6 draws the BER with respect to the traffic load η for both the scheduling policies, for $\sigma_\tau = 1.5\mu$s, SINR=5dB and SNR=6dB. For this correlated fading environment, we can conclude that the interference coordination policy provides the best performance for moderate system load, while interference randomization is to be preferred for heavy traffic load. Notice that the performance of the genie and the conventional decoders are quite similar here with respect to [6]. This happens because the diversity introduced by the multipath fluctuations over the frequency domain reduces the effects of the lack of instantaneous interference information; furthermore, the present analysis does not account for the shadowing.

V. Conclusions

In this paper an analytical framework has been derived to assess the performance of MIMO-OFDMA LTE systems with two different interference mitigation scheduling techniques over realistic frequency-selective channels. The analysis was carried out for varying degree of channel correlation over the subcarriers, ranging from the frequency flat to the ideal case of uncorrelated fading. In all the cases, reuse partitioning is shown to achieve the best performance for moderate traffic loads, while interference randomization should be the preferred choice for high traffic loads.

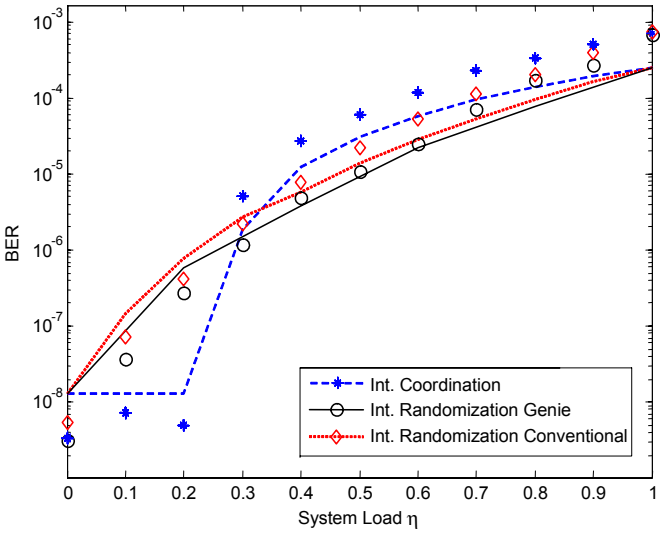

Fig. 6. Analytical (line) and simulated (marker) BER vs system load η.

References

[1] 3GPP Technical Report TR 25.814, "Physical layer aspects for the evolved Universal Radio Access (E-UTRA)," Release 7, 2006.

[2] 3GPP Technical Specifications TS 25.212, "Multiplexing and channel coding," Release 7, 2006.

[3] H Ekstrom et al., "Technical solutions for the 3G long-term evolution," *IEEE Communication Mag.*, vol 44, pp. 38-45, March 2006.

[4] D. Molteni, M. Nicoli, R. Bosisio, L. Sampietro, "Performance analysis of multiantenna WiMax systems over frequency selective fading channels," *Proc. IEEE PIMRC '07*.

[5] G. Fodor, "Performance Analysis of a Reuse Partitioning Technique for OFDM Based Evolved UTRA," *Proc. IEEE IWQoS*, June 2006.

[6] R. Bosisio, U. Spagnolini, "Interference coordination vs. interference randomization in multicell 3GPP LTE system," *Proc. IEEE WCNC '08*.

[7] E. G. Larsson and P. Stoica, *Space-Time Block Coding for Wireless Communications*, Cambridge University Press, 2003.

[8] J.G. Proakis, *Digital Communications*, McGraw Hill 2001.

[9] M. Simon, M. Alouini, *Digital Communication over Fading Channels*, Wiley, 2000.

[10] M. Alouini, A. Abdi, M. Kaveh, "Sum of gamma variates and performance of wireless communication systems over Nakagami-fading channels," *IEEE Trans. Vehic. Tech.*, vol. 50, pp. 1471-1480, Nov. 2001.